Nuclear Instruments and Methods in Physics Research A 1069 (2024) 169865

Contents lists available at ScienceDirect

Nuclear Inst. and Methods in Physics Research, A

journal homepage: www.elsevier.com/locate/nima

Design and commissioning of a two-harmonic pre-buncher for extended bunch spacing at LEAF

Yu Tang [a,b], Yao Yang [a,*], Bo Zhang [a], Yuhan Zhai [a], Zehua Jia [a], Xianwu Wang [a], Zhiming Hu [a,c], Jiao Xu [a,b], Libin Li [a], Long Jing [a], Yucheng Feng [a], Houqin Wang [a], Liepeng Sun [a], Liangting Sun [a], Xiaodong Tang [a], Hongwei Zhao [a]

[a] Institute of Modern Physics, Chinese Academy of Sciences, Lanzhou 730000, China
[b] University of Chinese Academy of Sciences, Beijing 100039, China
[c] Lanzhou University, Tianshui South Road No. 222, Lanzhou 730000, China

A B S T R A C T

The Low Energy Heavy Ion Accelerator Facility (LEAF) is a low-energy, high-intensity heavy-ion linear accelerator facility at Institute of Modern Physics (IMP) for multidiscipline research. The beam bunch repetition rate coincides with the LINAC frequency of 81.25 MHz, resulting in a 12.3 ns period. However, in the context of certain nuclear physics experiments, a longer bunch spacing is deemed essential for the precise detection of experimental products. To address this need, a strategy to extend the bunch spacing to 98 ns has been proposed by integrating a pre-buncher operating at a fundamental frequency of 10.156 MHz before the radio-frequency quadrupole (RFQ) in conjunction with a fast chopper in the medium energy beam transport (MEBT) system. The pre-buncher is a pivotal component in enabling a greater beam current at the target, surpassing the capability of employing a chopper alone. To enhance the bunching efficiency, the pre-buncher operates with two frequencies: the fundamental frequency of 10.156 MHz and its first sub-harmonic of 20.3125 MHz, each of which is produced by a coaxial resonator. This paper describes the design, manufacture, off-line testing, and beam commissioning of the pre-buncher.

1. Introduction

LEAF is a complex linear accelerator (LINAC) specifically designed for accelerating low-energy, high-intensity heavy ions, enabling research in diverse fields such as material irradiation and nuclear astrophysics experiments [1]. The facility offers heavy ion beams with a mass-to-charge ratio (A/q) ranging from 2 to 7 and adjustable energies between 0.3 MeV/u and 0.7 MeV/u. As shown in Fig. 1, LEAF is mainly composed of an electron cyclotron resonance ion source (ECRIS), a low energy beam transport (LEBT), an 81.25 MHz continuous wave (CW) RFQ accelerating ions to 0.5 MeV/u, an 81.25 MHz drift tube linac (DTL) providing adjustable energies from 0.3 MeV/u to 0.7 MeV/u, a MEBT, and experimental terminals. In order to achieve the minimum output longitudinal emittance and reduce the vane length, an external pre-buncher was used upstream of the RFQ. This multi-harmonic pre--buncher functions at a sub-harmonic frequency of 40.625 MHz [2], which is precisely half of the LINAC's fundamental frequency. Its primary objective is to enhance the longitudinal beam matching and improve the efficiency of RFQ acceleration. The RFQ, with an injection phase designed at −45°, selectively accepts well-bunched core particles for subsequent acceleration to avoid capturing a small fraction of particles in the tails of the distribution.

The original design of LEAF mandated a beam bunch repetition rate of 81.25 MHz at the target, resulting in a 12.3 ns time interval between bunches. However, this repetition rate has raised concerns among nuclear scientists, highlighting the need for a more distinct separation between bunches. Typically, by introducing a beam-free time interval of approximately 100 ns between bunches, it becomes possible to avoid overlapping time spectra of consecutive beam pulses, thereby enabling the implementation of time-of-flight (TOF) techniques [3,4]. Various techniques have been employed by several experimental facilities to impose specific temporal structures and achieve similar beam properties. For example, accelerator facilities like the Argonne Tandem Linear Accelerator System (ATLAS) [5], the Isotope Separated Accelerator (ISAC) [6], and the Facility for Rare Isotope Beams (FRIB) [7] are capable of achieving beam bunch spacings in the range of tens of nanoseconds. At experimental facilities such as the Soreq Applied Research Accelerator Facility (SARAF) [8], the Frankfurt Neutron Source at the Stern-Gerlach-Zentrum (FRANZ) [9], and the Rare Isotope Accelerator Complex for On-Line Experiments (RAON) [10], the beam repetition time can range from a few microseconds to tens of microseconds.

* Corresponding author.
E-mail address: yangyao@impcas.ac.cn (Y. Yang).

https://doi.org/10.1016/j.nima.2024.169865
Received 7 July 2024; Received in revised form 28 August 2024; Accepted 7 September 2024
Available online 7 September 2024

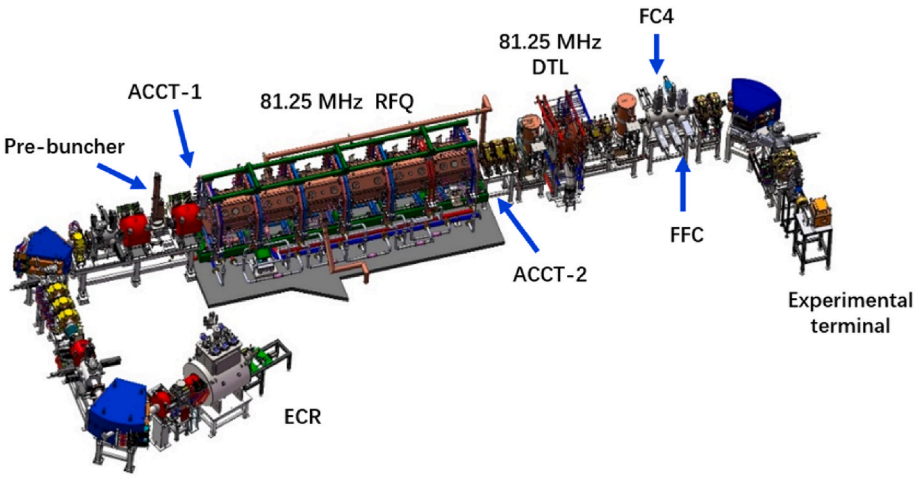

Fig. 1. Schematic view of LEAF facility.

To extend the bunch spacing for LEAF, a strategy has been proposed that involves a pre-buncher operating at a sub-harmonic frequency of 10.156 MHz (a factor of 8 below the LINAC's fundamental frequency) before the RFQ, in conjunction with a fast chopper in the MEBT. The pre-buncher is devoted to maximizing particle conservation because merely incorporating a chopper after the RFQ to discard 7 out of 8 bunches would result in about 85% beam loss. The pre-buncher enables the formation of main bunches separated by a 98.4 ns time interval, with seven satellite bunches interspersed between them. The fast chopper after the RFQ selectively suppresses the satellite bunches while preserving the main bunches, resulting in a larger current increment at the target.

Two types of pre-bunchers are commonly used: one that relies on a resonant circuit and the other that utilizes a resonant cavity. Several existing pre-bunchers follow the traditional resonant circuit setup involving the tank circuit and electronics [11] to achieve bunch voltage in the gap. Examples include the dual-gap pre-buncher at the Heavy Ion Research Facility of Lanzhou (HIRLF) [12] and the four-harmonic one-gap pre-buncher at ATLAS [13]. Unfortunately, this technique of generating sawtooth waveforms makes it difficult to manage the substantial powers needed for effective bunching of ion beams with a high A/q ratio, primarily due to thermal concerns [5]. For the injection system of LEAF, a coaxial resonator-based pre-buncher is favored, as ions with A/q = 7 require a bunching voltage of about 5 kV, which is regarded as risky for circuit-based approaches [5]. Some coaxial resonator pre-bunchers have already been developed, with examples including those at the Positive Ion Accelerator for Very Low Energy (PIAVE) Linac [14], the National Superconducting Cyclotron Laboratory (NSCL) [15], ATLAS [5], and the Beijing Isotope-Separation-On-Line Neutron-Rich Beam Facility (BISOL) [16]. Inspired by these examples, our design utilizes a quarter-wave resonator (QWR) cavity-based structure with a coaxial resonator configuration.

This paper details the design and commissioning of the pre-buncher, consisting of four sections describing (i) the beam dynamics performance, (ii) the RF design and multiphysics analysis, (iii) the manufacture and RF testing, and (iv) the experimental results of the pre-buncher.

2. Beam dynamics simulations

2.1. The principle of pre-bunching for an RFQ

Theoretically, an idealized voltage formed in a pre-buncher would have a pure sawtooth waveform with a perfectly linear ramp and an instantaneous return to the starting voltage at the end of each period [17]. To produce the desired sawtooth wave voltage, the technique of Fourier synthesis is utilized, which combines a series of sinusoidal waves at integer multiples of the fundamental frequency to form a sawtooth wave as a function of time [18]. The sawtooth wave voltage form can be expressed by using the Fourier expansion:

$$V_{(t)} = V_m(\sin \omega t - 0.40 \sin 2\,\omega t + 0.18 \sin 3\,\omega t - \ldots + C_n \sin n\omega t) \quad (1)$$

It is well established that the greater the number of harmonics, the better the fit to the ideal sawtooth wave [19]. Typically, this waveform is usually approximated by using its first 2–4 Fourier components, generated through a resonant cavity or circuit. As a result, a "tail" area appears at both ends of a period. When the pre-buncher operates at a subharmonic frequency of the accelerator, it leads to the formation of satellite bunches since particles in the tail area can enter different acceptance windows.

Fig. 2 illustrates the concept of bunching. In the pre-buncher, the leading particles encounter a decelerating voltage, while the lagging particles experience an accelerating voltage. In the distance from the pre-buncher to the RFQ, beam energy remains constant, but the relative phases change accordingly. Most of the beam converges within a narrow

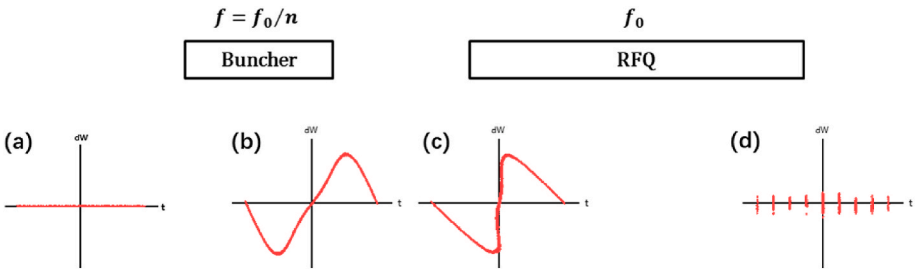

Fig. 2. The longitudinal beam distribution evolution along the beamline: (a) before the pre-buncher, (b) at the exit of pre-buncher, (c) at the entrance of RFQ, (d) after the RFQ.

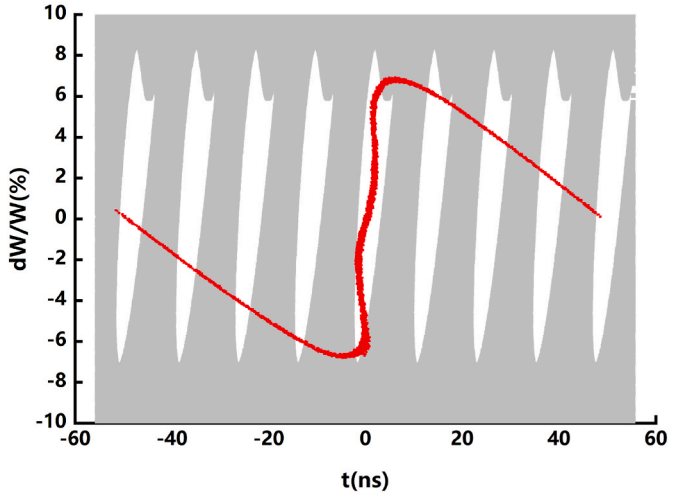

Fig. 3. A plot of the time and energy distribution of a simulated beam bunched at 10.156 MHz (shown in red), the white regions indicate the acceptance windows for an RFQ operating at 81.25 MHz.

time spread to fit the RFQ's longitudinal acceptance at the entrance, and unbunched beam particles in the tail areas may either end up in satellite RF buckets or get lost.

To accommodate LEAF users' requirement for bunches approximately 100 ns apart, a pre-buncher running at 10.15625 MHz is used to structure main bunches with a temporal separation of 98.4 ns. Fig. 3 provides a visual representation of pre-bunching at the 8th subharmonic of the RFQ. In this figure, white regions correspond to the RFQ's longitudinal phase space acceptances, while red dots depict the particle distribution. Each buncher period contains eight longitudinal acceptance windows, which results in the formation of seven satellite bunches alongside the primary ones.

2.2. Beam dynamic simulation with the gap electric field of the pre-buncher

The designed ion beam is ^{238}U with a charge state of 34. The ion beam is injected into RFQ at an energy of 14 keV/u, with a beam energy spread of 0.05%. Throughout the study, the beam current is expected to be approximately equal to 100 euA. Fig. 4 illustrates the transverse envelope of the beam. The pre-buncher is situated 1.1 m before the RFQ. A solenoid upstream of the buncher forms a narrow beam waist at the buncher's center, leading to relatively small beam envelopes in both transverse directions. Another solenoid placed after the buncher is employed for transverse matching with the RFQ.

For this segment of the beam transport calculations via the TRACK code [20], we assumed, for model simplicity, that the pre-buncher possesses only the central field in the gap between the electrodes, as illustrated in Fig. 5. Exhaustive simulations with different harmonic combinations (10.156 MHz, 10.156 MHz +20.3125 MHz, and 10.156 MHz +20.3125 MHz + 30.468 MHz) were performed to identify the optimal coefficients for a certain count of harmonics. Fig. 6 depicts longitudinal phase space distributions at the input of the RFQ under these situations when an optimal bunching efficiency (bunching efficiency actually corresponds to the accelerating efficiency of the RFQ, determined by comparing particles entering the RFQ acceptance region to the total particles within one RF buncher period) is achieved. The calculated effective modulated voltages of the harmonics and bunching efficiency for four different cases are listed in Table 1. The data indicates that the introduction of a pre-buncher, even operating solely at the fundamental frequency, can amplify the bunching efficiency by 20% compared to not having a pre-buncher. Furthermore, the bunching efficiency is increased by 26% when utilizing both the first and second harmonics. However, the incorporation of three harmonics leads to a mere 1% enhancement in bunching efficiency over the engagement of two harmonics, attributed to the constrained energy spread acceptance of the RFQ (see Fig. 6). Hence, to optimize RF and control systems, a dual-harmonic setup is chosen for the pre-buncher.

Fig. 7 shows the distribution of particle numbers within bunches at the RFQ exit in scenarios with and without pre-bunching. Employing a pre-buncher leads to around 81.6% of accelerated particles being collected in the primary bunch, while 18.4% of accelerated particles are distributed among satellite bunches. Conversely, without a pre-buncher, each bunch accommodates a scant 12.5% of accelerating particles. If an RF chopper is installed in the MEBT to establish a 98.4 ns interval amid two main bunches, the dual-frequency pre-buncher configuration yields a current gain of 6.5 in the target.

2.3. Beam dynamic simulations with the gap and leakage electric field of the pre-buncher

Besides the central field in the electrode gap, there exist leakage fields beyond the electrodes along the beam passage, as shown in Fig. 8. To assess the influence of the leakage field of each harmonic, it is necessary to calculate the relevant transit time factor (TTF), which is defined as the ratio of the energy acquired in the time-varying RF field to the energy gained in a DC field with voltage $V_0 \cos \varphi$ [21], and can be

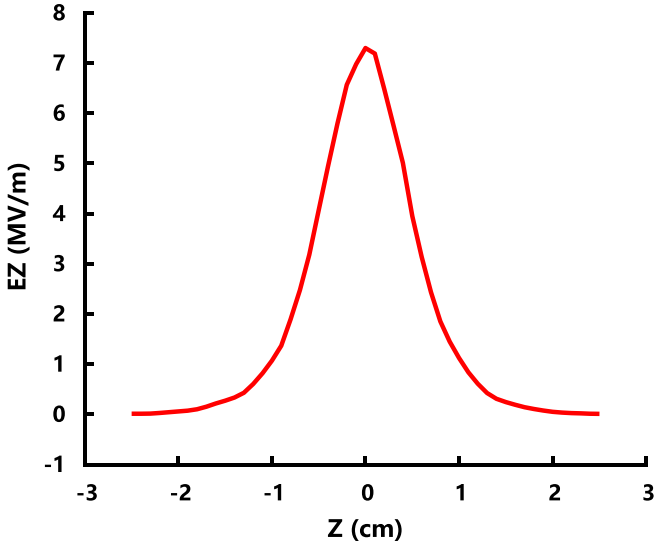

Fig. 5. The longitudinal electric field distribution along the beam axis in the gap at radial position r = 0 mm.

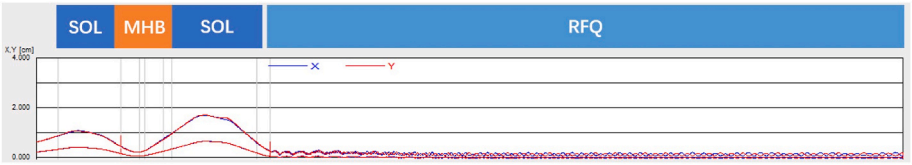

Fig. 4. The transverse beam transmission along the beam line.

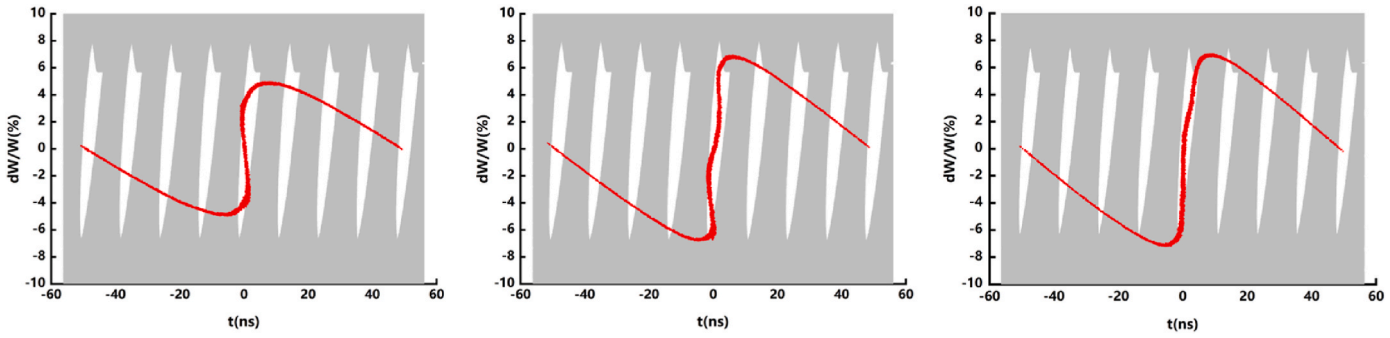

Fig. 6. Modulated beam particle distributions vs. RFQ longitudinal acceptance.

Table 1
The modulated voltages and bunching efficiency under different harmonic combinations, where U_1, U_2, and U_3 represent the voltage amplitudes of the fundamental, second harmonic, and third harmonic frequencies, respectively.

Harmonic	U_1	U_2	U_3	Bunching Efficiency
Without pre-buncher	0	0	0	50%
1-harmonic	5.15 kV	0	0	70%
2-harmonics	6.4 kV	1.6 kV	0	75.8%
3-harmonics	6.5 kV	1.8 kV	0.18 kV	77%

The calculations indicate that the uranium beam necessitates a 1st harmonic voltage (U_1) of 6.4 kV and a 2nd harmonic voltage (U_2) of 1.6 kV to reach the highest bunching efficiency. Gleaning insights from the ATLAS experience, a lumped circuit multi-harmonic buncher (MHB) stumbles to operate efficiently at the necessary voltage amplitude of 6.2 kV due to thermal challenges [5], incentivizing us to opt for the coaxial resonator cavity solution.

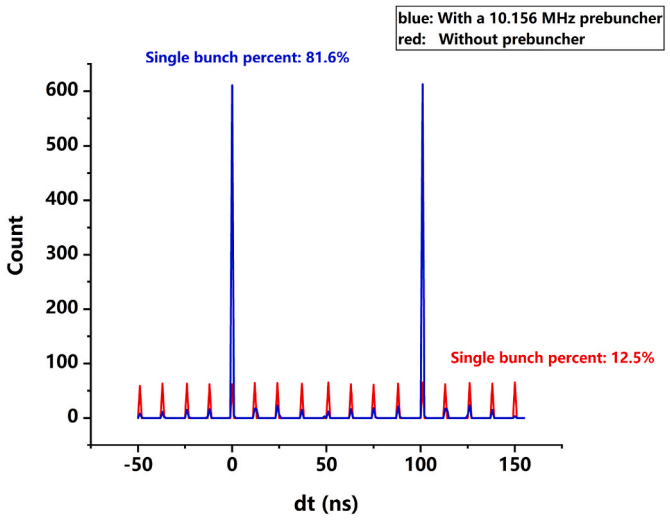

Fig. 7. The distribution of particle numbers within bunches at the RFQ exit in scenarios with and without bunching.

estimated by the following approximation:

$$T = \frac{\int_{-\frac{L}{2}}^{\frac{L}{2}} E(0,z)\cos\frac{2\pi z}{\beta\lambda}\,dz}{\int_{-\frac{L}{2}}^{\frac{L}{2}} E(0,z)\,dz} \tag{2}$$

Where L is the axial distance containing the electric field. $E(0,z)$ is the z component of the electric field in the direction parallel to the beam axis at radial position $r = 0$. λ is the wavelength. β is the nominal relativistic velocity (0.0054826 with a beam energy of 14 keV/u).

Fig. 9 displays the TTF variations with the RF frequency when the spacing between the electrodes is set to 4 mm and the inner and outer apertures of the electrodes are 16 mm and 30 mm, respectively. The trends in the graphs signify that TTF values escalate as frequency decreases, and the effect of the leakage electric fields becomes significant due to the high TTF values at lower frequencies: 0.64 for the 10.156 MHz and 0.34 for the 20.3125 MHz. Nevertheless, by modifying the length of the electrode, it is feasible to efficiently utilize the advantageous influence of the leakage fields.

As the leakage field and central gap field exhibit opposite polarities as illustrated in Fig. 8, adjusting the distance between their centers to an odd multiple of $\beta\lambda/2$ effectively utilizes the leakage field for beam bunching. The configuration induces the RF phase advance by an odd multiple of π as the beam synchronizes with the RF field in each gap. This arrangement allows the incorporation of the outer gap voltage into the bunching voltage, thereby decreasing the voltage demand in the central gap and subsequently reducing power consumption. Fig. 10 showcases the optimally configured electrode structure in accordance with this principle. The first harmonic has an electrode length (Elec1) of 61 mm, while for the second harmonic, the electrode length (Elec2) is set to 107 mm, given the impracticality of using the electrode length for $\beta\lambda_2/2$ due to shortness. The wide outer gap allows the lengths of the two electrodes to remain at 61 mm and 107 mm, providing adequate space for particles to traverse the electrodes and proceed to the next gap as the electric field phase shifts by an odd multiple of π. Table 2 presents the requisite central gap voltages for ions with a charge-mass ratio of 1/7 when the two harmonics being loaded. The exploitation of the leakage field effectively curtails the amplitude of central gap voltages, particularly for the first harmonic, whose gap voltage decreases by 1.7 times compared to scenarios without leakage field utilization.

To enhance the utilization of the leakage field, the outer gap length of the first harmonic was decreased to 5 mm by introducing a drift tube on the end plate and extending the electrode length of the first harmonic, as illustrated in Fig. 11. Fig. 12 displays the distribution of the E_z component of the first harmonic along the beam axis in the modified model. This alteration raises the TTF of the first harmonic's leakage field from 0.64 to 0.97, leading to a decrease in the requisite central gap voltage from 2.94 kV to 2.55 kV.

However, to preserve the π-mode electrode structure, the electrode length Elec1 was extended from 61 mm to 81 mm (precisely equal to $\beta\lambda_1/2$), leading to a three-fold voltage decrease in both the outer and central gaps of the first harmonic at the same power assumptions. As a result, the power needed for the first harmonic surged from 160 W to 939 W to preserve the same bunching efficiency (with only the first harmonic being loaded). This deviated from our original goal of power reduction, consequently maintaining the electrode structure configuration with short electrodes and wide outer gaps.

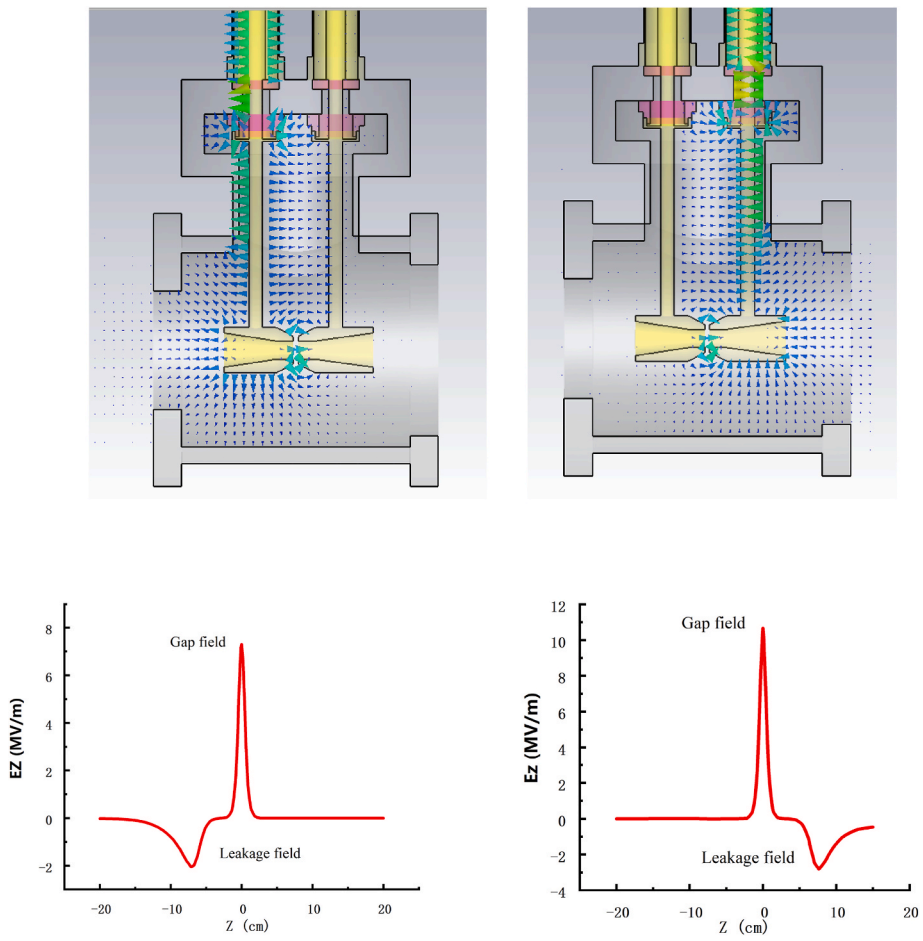

Fig. 8. The electric field array plot in the chamber from an axial cut plane (top) and the distribution of the E_z component along the cavity axis of the 1st harmonic (10.156 MHz) (left) and 2nd harmonic (20.3125 MHz) (right).

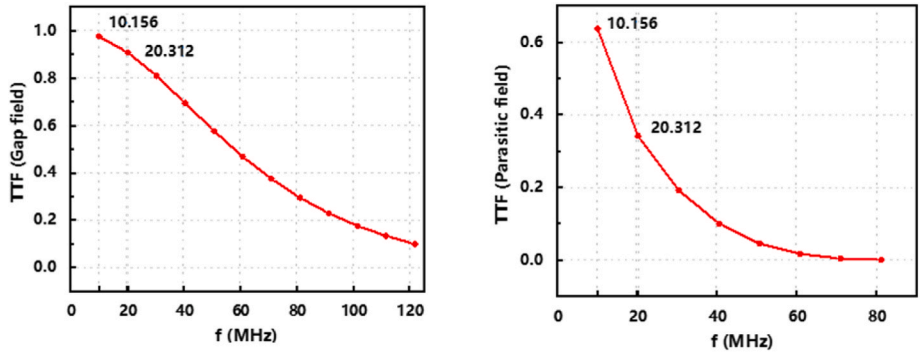

Fig. 9. The TTFs as a function of the RF frequency calculated with the gap field (left) and leakage field (right) under the same electrode structure.

3. RF design and multiphysics analysis

3.1. RF design

The electromagnetic design of the cavity was carried out using the CST Studio Suite [22]. Fig. 13 illustrates the conceptual RF structure along with specific chamber details. The pre-buncher employs two drift tubes as gridless electrodes. Each electrode, directly linked to the resonators' inner conductors, is housed in a cylindrical vacuum chamber that acts as an open boundary for the coaxial resonators. The beam dynamics necessitate that the electrodes' lengths be fixed at 61 mm and 107 mm, respectively. To uphold a high transit time factor, a 4 mm separation between the electrodes has been maintained. The diameter of the electrode's smaller aperture is set at 16 mm to facilitate the passage of an intense heavy ion beam.

Since we have similar research goals of beam spacing and high beam voltage as ANL, we opted for the same buncher type as Argonne [5]. The two frequencies are produced by two quarter-wave resonators (QWR), with one end being short-circuited and the other left open-circuited. However, unlike the buncher at Argonne Laboratory, to ensure compatibility with the limited space of the LEAF beamline and keep costs low, the resonators adopt the EIA 1–5/8″ standard transmission line. The transmission lines' lengths approach the ideal $\lambda/4$ length, being approximately 7.3 m for the first harmonic and 3.5 m for the second, to

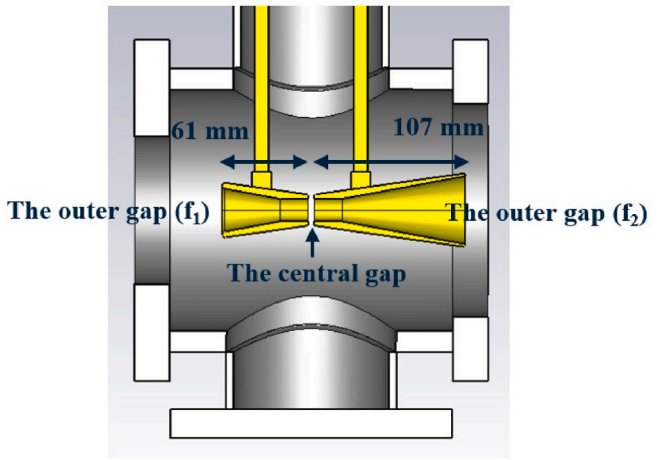

Fig. 10. The optimized π-mode electrode structure consisted of two asymmetrical electrodes and three bunch gaps.

Table 2
The comparison of simulation results under different conditions. Elec1 refers to the drift tube length connected to the resonator producing the first harmonic. Elec2 refers to the drift tube length connected to the resonator producing the second harmonic.

Parameters	With gap and leakage field	With gap field
Elec1/mm	61 ($\beta\lambda_1$ /2)	–
V_{f1}/kV	3.71	6.41
Elec2/mm	25 ($\beta\lambda_2$/2)/107 (3$\beta\lambda_2$/2)	–
V_{f2}/kV	1.27	1.63

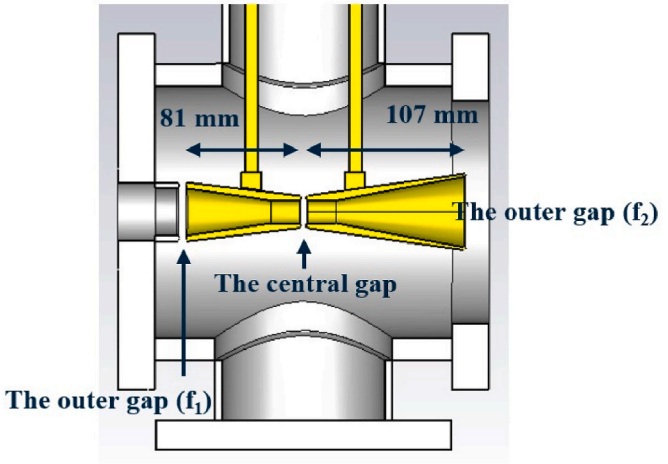

Fig. 11. The modified electrode structure.

achieve the desired resonance frequency. As depicted in Fig. 13, the resonators are vertically folded to improve system compactness.

Each resonator employs a magnetic coupler using loops to supply RF power. The coupler loops, positioned in a high magnetic field for each resonance mode, remain orthogonal to the magnetic field. The coaxial-to-cavity coupling factor is defined as $\beta = Q_0/Q_{ext}$ [23]. Maximum power is coupled into the cavity at $\beta = 1$, known as critical coupling. The RF coupling loop dimensions are designed to ensure coupling strength slightly above critical for each harmonic, catering for scenarios of possible insufficient coupling in practice. The coupler loops ought to be appropriately folded into turns owing to the space constraint between the outer and inner pipes, as depicted in Fig. 14. Couplers for the first

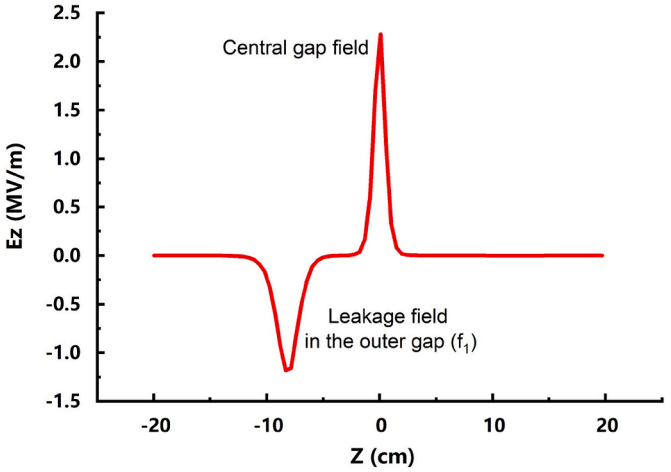

Fig. 12. The distribution of the E_z component along the cavity axis of the 1st harmonic (10.156 MHz) in the modified model.

and second harmonics share a similar design, differing mainly in loop area and placement. Relevant coupler parameters are detailed in Table 3. Two RF probes, having the shape of a 7 × 15 mm single-turn loop, are located near their respective RF power couplers for monitoring the amplitude of each harmonic.

Typically, despite meticulous design, the machining tolerances and brazing process during fabrication may cause deviations from the intended structure frequency. Additionally, the heat generated during high-power operation can lead to frequency drift. Consequently, the cavity needs to be tuned accordingly. Two types of tuners are used: coarse tuners and fine tuners. Coarse tuning is accomplished by adjusting the sliding plunger's position at the resonator's end, equivalent to modifying the resonator's length. The predicted coarse frequency tuning ranges of 385 kHz for the 10.156 MHz (abbreviated as "10 MHz" later) and 1032 kHz for the 20.3125 MHz (abbreviated as "20 MHz" later) over the full plunger movement (from + 100 mm to −100 mm) are capable of dealing with the frequency shift. Fine-tuning is achieved using a 16-mm-diameter screw tuner on the outer conductor of each resonator. The fine tuners are positioned in proximity to the maximum electric field strength in the resonators to achieve a frequency adjustment range as wide as possible. The principal design parameters of the pre-buncher are summarized in Table 4.

3.2. Multiphysics analysis

Introducing high-power feed-in can create a heat load in the cavity, potentially causing mechanical deformation and consequently altering the resonator's eigen frequency. As a result, a coupled RF-thermal-mechanical analysis is necessitated. The subsequent multiphysics analysis was conducted using CST MWS via these steps: Firstly, the thermal load is evaluated using the thermal solver based on the electromagnetic field distribution from the Eigenmode solver. By importing the calculated maximum RF power (220 W for the 10 MHz resonator and 26 W for the 20 MHz resonator) into the cavities. Under natural air convection, it is observed that RF heating is mostly focused on the inner conductor, with peak temperatures of 107 °C (10 MHz) and 47 °C (20 MHz) measured near the back end of the inner conductors, respectively. Subsequently, the steady-state temperature distributions are exported to the structure solver to compute structural deformations. The inner conductor of two resonators undergoes maximum deformations of 2.75 mm and 1.44 mm, respectively. The structural deformations are then sent to the Eigenmode solver for frequency shift assessment. The first and second harmonic frequencies shift by 5.9 kHz and 5.18 kHz, respectively, as a result of deformations.

To relieve RF heating and ensure reliable operation of the pre-

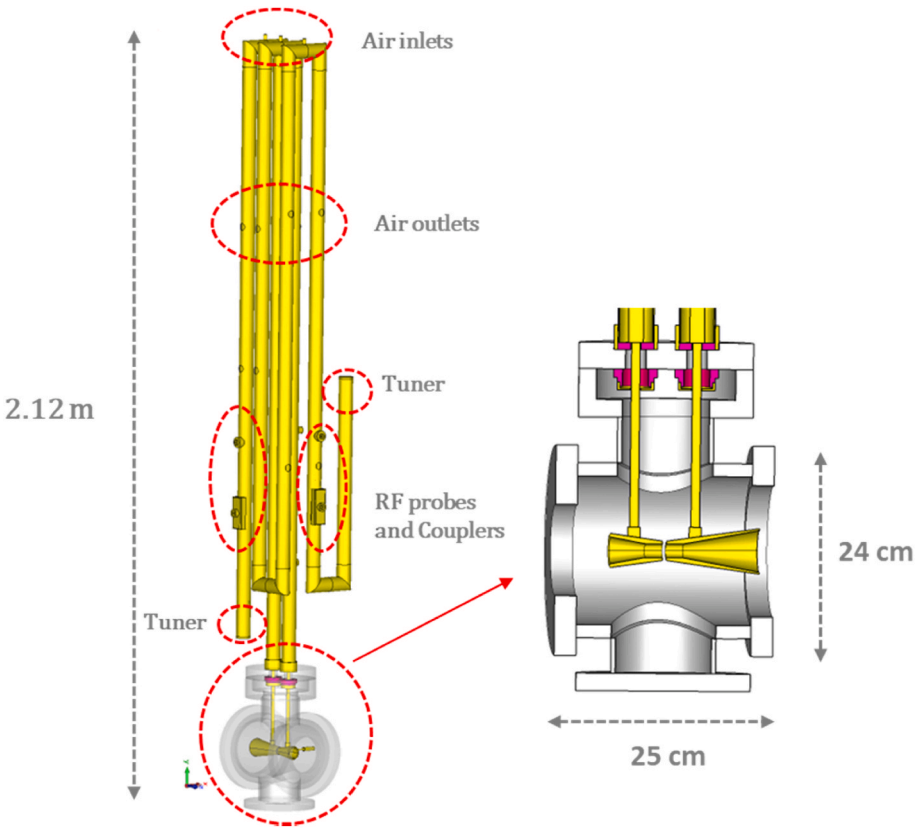

Fig. 13. The conceptual RF structure of the pre-buncher and the details of the chamber.

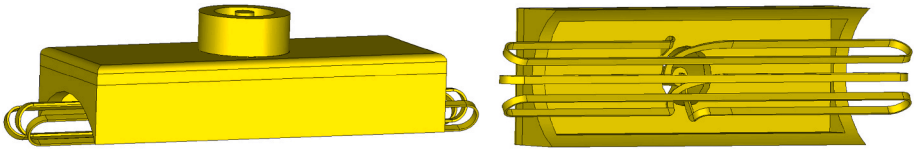

Fig. 14. RF models of the magnetic coupler using loops for the 1st harmonics.

Table 3
Relevant coupler parameters of the 1st and 2nd harmonics.

Harmonic	1st	2nd
Loop area (cm^2)	27	11.3
Q_0	480	670
Q_{ext}	446	637
$\beta = Q_0/Q_{ext}$	1.07	1.05

Table 4
Simulated parameters of the pre-buncher.

Harmonic	10.156 MHz	20.3125 MHz
The resonator length	7.33 m	3.5 m
Quality Factor	480	670
Coarse tuning range	385 kHz	1032 kHz
Fine tuning range	12 kHz	29 kHz
Maximum effective V_{max}	3.71 kV	1.27 kV
Maximum RF power P_{max}	220 W	26 W

buncher, a forced air-cooling scheme is proposed by introducing pressurized air into the resonators via upper air inlets and punching holes in the outer conductor as air outlets (as shown in Fig. 13). In the simulation, the temperature of the pressurized air was set at 20 °C, and the air convection heat transfer coefficient of 30 W/(m^2K), estimated by the air velocity of 12 m/s, was applied to the inner conductors' surfaces. The results show that the peak temperatures of the inner conductors for the two resonators drop below 44 °C and 28 °C, and the maximum deformations are reduced to 0.46 mm and 0.3 mm, respectively. These deformations cause frequency shifts of $\Delta f_1 = 1.6$ kHz for the 10 MHz resonator and $\Delta f_2 = 1.06$ kHz for the 20 MHz resonator, which fall within the fine-tuners' adjustment range.

4. Manufacture and RF testing

4.1. Manufacture of the pre-buncher

The mechanical design of the pre-buncher benefits from the experience of the multi-harmonic bunchers at LEAF [2] and ATLAS [5]. Fig. 15 shows the schematic engineering drawing and a photograph depicting the complete assembly. Considering the limited installation space and manufacturing costs, the pre-buncher utilizes standard EIA 1–5/8" coaxial frigid transmission lines as the resonators. Ensuring mechanical stability and operational simplicity, the resonators, extending several meters, are built from multiple feeder tube segments joined by elbows to maintain an overall height of approximately 2 m. One end of the outer conductors of the resonator is directly inserted into bronze sleeves welded to a CF150 flange, while the inner conductors are linked to the

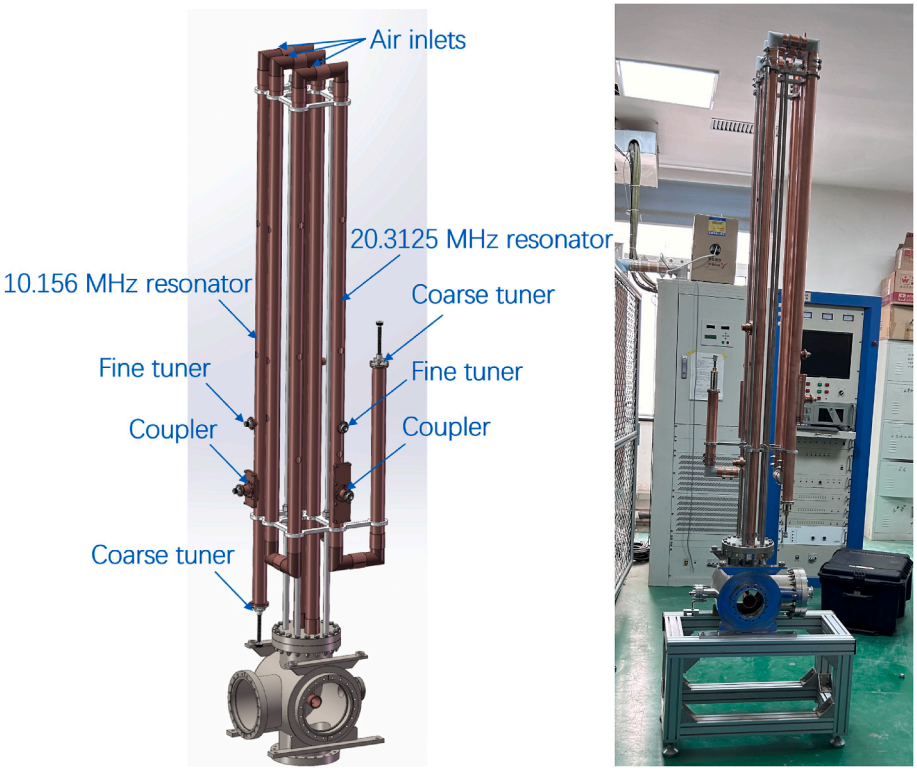

Fig. 15. The schematic engineering drawing (left) and the complete assembly of the pre-buncher (right).

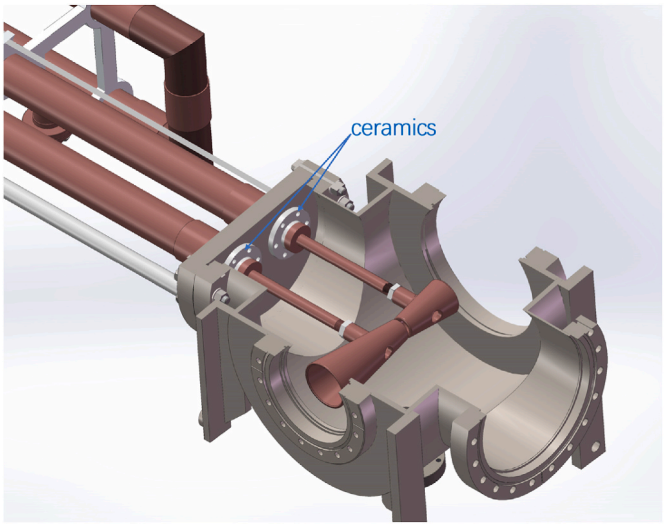

Fig. 16. Internal structure of the chamber.

electrodes through inserts. At the opposite end, the inner and outer conductors are short-circuited via the plungers, which serve as coarse tuners. The fine tuners, as described above, are copper screws with a diameter of 16 mm on the outer conductor. Insulation between the inner and outer conductors of the resonator and vacuum sealing of the chamber are achieved by welding ceramic insulators to copper flanges, and then brazing them to the inner conductors, as illustrated in Fig. 16. Electrode height is adjusted using threads, while the alignment of the two electrodes is concentrically accomplished through the utilization of a concentric axis and a measuring arm. Three air inlets on the top of resonators are connected to blow tubes for forced air cooling. Additionally, several air outlets are distributed on the resonators to promote air circulation and allow for temperature measurements. Additional components on the resonators include couplers and pick-ups. The power couplers are made of copper assemblies with *N*-type connectors, and their outer bodies are brazed onto the outer conductors. The outer section of the coupler is rectangular for easier installation of the coupler loop. Moreover, the couplers are equipped with an insertion depth adjuster and a coupling loop angle adjuster (see Fig. 17).

4.2. RF testing

After assembly, the cold mode measurement of the pre-buncher was carried out using a vector network analyzer (VNA). The frequencies of 10.156 MHz and 20.3125 MHz were established via adjustment of both coarse and fine tuners, and the coupling of the two harmonics is finely tuned to critical coupling by adjusting the depth and angle of the coupling loop. At the 10.156 MHz frequency, we measured an RF reflection coefficient S11 of −32 dB and an unloaded quality factor of 321, representing 67% of the design value. Similarly, at the 20.3125 MHz frequency, a reflection coefficient S11 of −39 dB and an unloaded quality factor of 470 were attained, accounting for 70% of the design unloaded quality factor value.

Subsequently, the pre-buncher was driven by a bespoke dual-frequency power amplifier to ascertain its stability under high power. The introduction of high-power feed-in will generate a substantial heat load within the cavity, necessitating an assessment of the buncher's heat dissipation capacity at elevated power levels. Given that the measured Q values deviate by 67% and 70% from the simulated ones, the feed powers for the two harmonics were correspondingly increased to 330 W and 40 W, respectively, to maintain the same effective bunching voltage for a beam with $A/Q = 7$. Since the RF heating is largely concentrated on the inner conductor, we can't measure the complete temperature distribution directly. However, the eigen frequency shifts were monitorable. After several hours of operation with forced air cooling, the cavities reached the condition of thermal equilibrium, and the eigen frequencies remained stable. The final frequency shifts freeze at 5.7 kHz for the 10 MHz resonator and 2.8 kHz for the other, respectively. It is

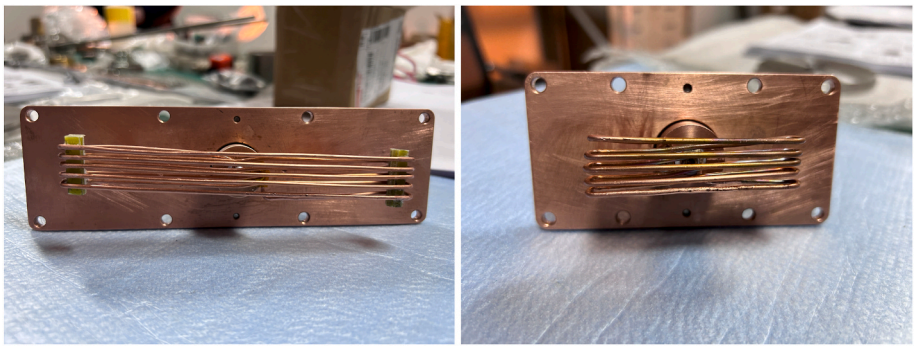

Fig. 17. Pictures of RF coupler for 10 MHz resonator (left) and 20 MHz resonator (right).

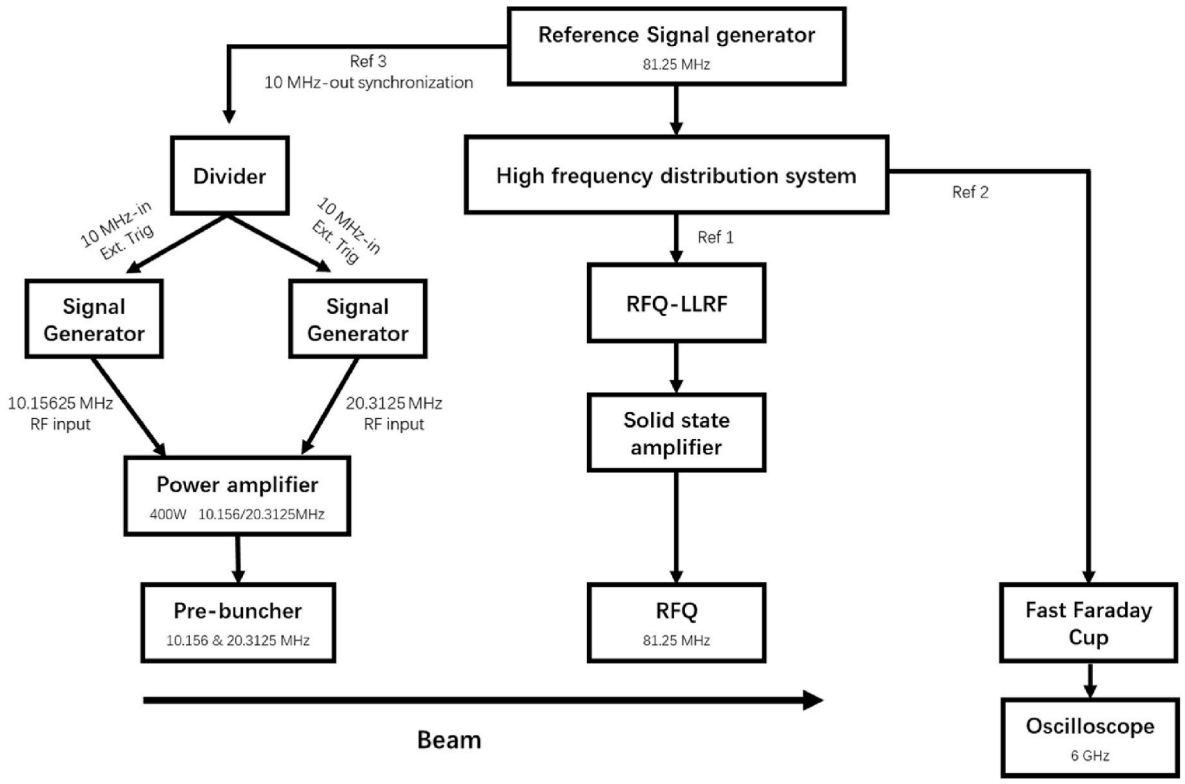

Fig. 18. Schematic diagram of the signal synchronization of this prebuncher connected to the accelerator rf control in the experiment setup.

easy to adjust the frequencies to the designed values only by fine tuners.

5. Beam commissioning

Fig. 18 illustrates signal synchronization between the pre-buncher and the accelerator RF control in the experimental setup. A signal generator supplies a synchronous reference signal at 81.25 MHz. At first, the signal is sent to both the RFQ and the fast Faraday using the high-frequency signal distribution system. The 10 MHz output synchronization signal from the signal source is divided using a power divider into two channels and then connected to two signal generators that provide RF input to the power amplifier of the pre-buncher in order to establish synchronization. Upon achieving signal synchronization among the pre-buncher and the RFQ, a beam test was conducted to evaluate the performance of the pre-bunching system using He^{+} beams with a beam current of 130 $e\mu A$. By careful optimization, the transmission efficiency of the RFQ exceeded 97%, which is defined as the ratio of beam currents measured by two AC current transformers (ACCT) located on either side of the RFQ. The RFQ achieves a maximum acceleration efficiency of 76.8% when the two harmonics of the pre-buncher are operating at the correct phase and amplitude. The acceleration efficiency is determined by the ratio of the beam currents at the Faraday Cup (FC4), which is positioned downstream of the MEBT quadrupole triplet, and ACCT-1, which is located upstream of the RFQ. The nonaccelerated particles would be overfocused and lost in the triplet focusing channel due to the widely different rigidity of the synchronous particles [1]. Table 5 compares the measured and simulated acceleration efficiencies (abbreviated as "acc-eff" later) under various operating conditions (without pre-buncher, with the fundamental frequency, with the first two

Table 5
The measured and simulated acceleration efficiencies under various MHB operation conditions.

Bunching mode	Measured acc-eff	Simulated acc-eff
w/o buncher	51%	50%
Pre-buncher (1st harmonic)	71.5%	70%
Pre-buncher (1st and 2nd harmonics)	76.8%	75.8%

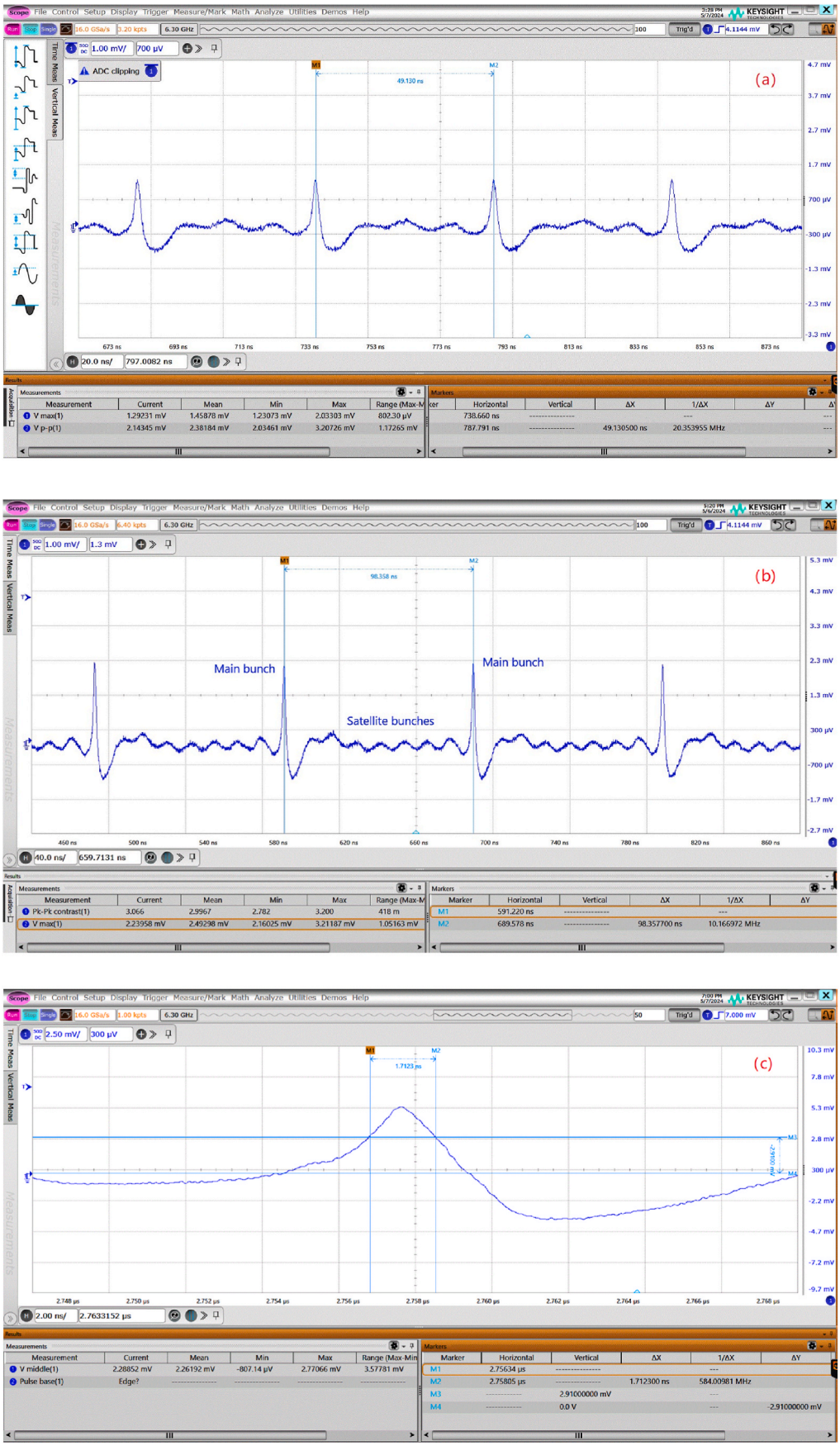

Fig. 19. Measured beam longitudinal time structure and FWHM of the main bunch by a Fast Faraday Cup.

harmonics).

The temporal structure of the beam is captured by a fast Faraday cup (FFC) after the RFQ, which has a time resolution of 50 ps. The signals were measured by a signal oscilloscope with a 6 GHz bandwidth and a 16 GSa/s sampling rate. Consistent with the simulation results, when the pre-buncher operates at a frequency of 20.3125 MHz, the time interval between primary bunches is close to 49.2 ns, with three satellite bunches observed between the main bunches as depicted in Fig. 19 (a). At a fundamental frequency of 10.156 MHz (as shown in Fig. 19 (b)), the interval between two main bunches is spaced at about 98.4 ns, and the trace indicates that there are seven satellite bunches between two adjacent main bunches. Fig. 19 (c) shows that the main bunch has a full width at half maximum (FWHM) of 1.7 ns when the pre-buncher is operated with two harmonics. The undershoot observed behind the beam bunch in the oscilloscope diagram is mainly caused by an impedance mismatch. The difficulty in achieving the standard 50Ω impedance for FFC during manufacturing results in visible overshoots at high incident particle number intensities. However, this negative rebound can be disregarded [24]. These results suggest that the pre-buncher has successfully established the desired beam time structure.

6. Summary

In order to separate the main bunches at around 100 ns and preserve as many particles as possible at the target, a specialized pre-buncher has been designed, fabricated, and tested with ion beams at LEAF. This pre-buncher operates at the 8th subharmonic of the RFQ frequency (10.156 MHz), integrating its subharmonic of 20.3125 MHz. The pre-buncher adopts two QWRs constructed from standard EIA 1–5/8" coaxial frigid transmission lines to generate the bunching voltage in a grid-less gap located between two accelerating electrodes. A notable characteristic of the pre-buncher is its unique electrode structure that functions in a π-phase advance mode, harnessing the leakage field to significantly decrease the total effective bunching voltage by 1.6 times. A detailed RF-thermal-mechanical analysis has been completed to ensure cavity operation, stability, and compatibility with the required power dissipation. Beam commissioning was carried out, revealing that the time interval between two primary bunches, as measured by FFC, is 98.4 ns, with individual satellite bunches separated by 12.3 ns. The successful operation of this pre-buncher serves as an excellent example of a buncher featuring low frequency, high voltage, cost-effectiveness, and compact size.

CRediT authorship contribution statement

Yu Tang: Writing – original draft, Methodology, Data curation. **Yao Yang:** Writing – review & editing, Funding acquisition, Conceptualization. **Bo Zhang:** Formal analysis. **Yuhan Zhai:** Investigation. **Zehua Jia:** Software. **Xianwu Wang:** Methodology. **Zhiming Hu:** Software. **Jiao Xu:** Visualization. **Libin Li:** Visualization. **Long Jing:** Investigation. **Yucheng Feng:** Investigation. **Houqin Wang:** Investigation. **Liepeng Sun:** Methodology. **Liangting Sun:** Project administration. **Xiaodong Tang:** Validation. **Hongwei Zhao:** Supervision.

Declaration of competing interest

The authors declare that they have no known competing financial interests or personal relationships that could have appeared to influence the work reported in this paper.

Data availability

Data will be made available on request.

Acknowledgments

This work is supported by the National Natural Science Foundation of China (Contracts No. 12375151 and 11427904), and the Scientific instruments and equipment development program of Chinese Academy of Sciences (Grant No. GJJSTD20210007).

References

[1] Y. Yang, L.T. Sun, Y.H. Zhai, et al., Heavy ion accelerator facility front end design and commissioning, Phys. Rev. Accel. Beams 22 (2019) 110101.
[2] Z.R. Wu, L.P. Sun, F. Qiu, et al., A new multi-harmonic buncher for the LEAF project, Nuclear Inst, And Methods in Physics Research A 1047 (2023) 167856.
[3] H. Makii, K. Mishima, M. Segawa, et al., Measurement system of the γ-ray angular distributions of the ^{12}C (α,γ) ^{16}O reaction, Nucl. Instrum. Methods Phys. Res. 547 (2005) 411.
[4] S.V. Kutsaev, et al., RF deflecting cavity for fast radioactive ion beams, EPJ Techniques and Instrumentation 7 (2020) 4.
[5] S.V. Kutsaev, A.Yu Smirnov, R. Agustsson, et al., Four-harmonic buncher for radioactive and stable beams switching at the ATLAS facility, Nucl. Instrum. Methods Phys. Res. A 905 (2018) 149.
[6] R. Laxdal, M. Pasini, and L. Root, Beam dynamics design study and beam commissioning of the ISAC two frequency chopper, in: Proceedings of LINAC2002, Gyeongju, Korea, p. 407. http://accelconf.web.cern.ch/accelconf/l02/PAPERS/TU441.PDF..
[7] A. C. Araujo Martinez, et al., Electromagnetic design of a compact RF chopper for heavy-ion beam separation at FRIB, in: Proceedings of NAPAC-2022, Lansing, MI. JACoW..
[8] A. Shor, et al., Fast chopper for single radio-frequency quadrupole bunch selection for neutron time-of-flight capabilities, Phys. Rev. Accel. Beams 22 (2019) 020403.
[9] C. Wiesner, et al., Experimental performance of an E × B chopper system, Phys. Rev. Accel. Beams 20 (2017) 020101.
[10] S.H. Moon, et al., Design study of a single bunch selection method for neutron TOF experiment at RAON heavy ion accelerator, J. Instrum. 17 (2022) T07007.
[11] A. Sarkar, et al., Single-gap multi-harmonic buncher for NSC pelletron, in: AIP Conference Proceedings, vol. 473, American Institute of Physics, 1999, 1.
[12] X.H. Zhang, Y.J. Yuan, J.W. Xia, Sawtooth-wave prebuncher with dual-gaps in Linac injector for HIRFL-SSC, Nucl. Instrum. Methods Phys. Res. A 879 (2018) 39–46.
[13] P.N. Ostroumov, V. N. Aseev, A. Barcikowski, Beam test of a grid-less multi-harmonic buncher, in: Proceedings of IEEE PAC2007, Albuquerque, pp. 2242-2244..
[14] A. Facco, F. Scarpa, V. Zviagintsev, The non-rfq resonators of the PIAVE linac, in: AIP Conference Proceedings, vol. 473, American Institute of Physics, 1999, 1.
[15] Daniel Alt, Design and Commissioning of a 16.1 MHz Multiharmonic Buncher for the Reaccelerator at NSCL, Michigan State University, 2016.
[16] M. Chen, Z.H. Peng, S.W. Quan, et al., Design study of multi-charge low energy beams transport for BISOL post accelerator, Nucl. Instrum. Methods Phys. Res. A 981 (2020) 164453.
[17] D. Alt, J. Brandon, D. Leitner, Preparation investigation for a low frequency prebuncher at REA, in: Proceedings of IPAC2014, Dresden, Germany, THPME051..
[18] F.J. Lynch, R.N. Lewi, et al., Beam buncher for heavy ions, Nucl. Instrum. Methods 159 (1979) 245.
[19] I.B. Magdau, M.A. Fraser, Beam dynamics feasibility study for an RFQ sub-harmonic pre-buncher at REX-ISOLDE, No. HIE-ISOLDE-PROJECT-Note-0015. available at: http://cds.cern.ch/record/1517514, 2013.
[20] V. Aseev, et al., TRACK: the new beam dynamics code, in: Proc. The Particle Accelerator Conference, 2005 TPAT02. Knoxville, USA.
[21] T.P. Wangler, RF Linear Accelerators, John Wiley & Sons, 2008.
[22] CST Microwave Studio, http://www.cst.com/.
[23] https://doi.org/10.48550/arXiv.1112.3201.
[24] Y. Yang, et al., Longitudinal emittance measurement for an external-bunching-based heavy-ion RFQ, Nuclear Inst, in: And Methods in Physics Research A, vol. 1029, 2022 166457.